Piezoelectric Electromechanical Coupling in Nanomechanical Resonators with a Two-Dimensional Electron Gas

A. A. Shevyrin,* A. G. Pogosov, A. K. Bakarov, and A. A. Shklyaev
Rzhanov Institute of Semiconductor Physics 13, Lavrentyev Avenue, Novosibirsk 630090, Russia, and Novosibirsk State University 2, Pirogov Street, Novosibirsk 630090, Russia
(Received 15 March 2016; published 30 June 2016)

The electrical response of a two-dimensional electron gas to vibrations of a nanomechanical cantilever containing it is studied. Vibrations of perpendicularly oriented cantilevers are experimentally shown to oppositely change the conductivity near their bases. This indicates the piezoelectric nature of electromechanical coupling. A physical model is developed, which quantitatively explains the experiment. It shows that the main origin of the conductivity change is a rapid change in the mechanical stress on the boundary between suspended and nonsuspended areas, rather than the stress itself.

DOI: 10.1103/PhysRevLett.117.017702

Most of the currently studied low-dimensional electron systems are fabricated from a two-dimensional electron gas (2DEG) embedded in a semiconductor bulk. A classical example of such a system is a 2DEG in GaAs/AlGaAs heterostructures. However, selective etching of a sacrificial layer (often called surface nanomachining) also gives us an opportunity to create a 2DEG embedded in a thin membrane freely suspended over a substrate [1]. The nanostructures fabricated from such membranes are mechanically moveable with their movement affecting electron transport and conductivity [2]. Such electromechanical coupling gives us an opportunity to probe mechanical motion at the nanoscale and it could be used to study interesting mechanical phenomena, such as "phonon lasing" [3] and the quantum-limited motion of an artificially made object [4]. Moreover, it opens up new prospects for studying nontrivial transport phenomena in a 2DEG under unusual conditions, namely, in the presence of additional mechanical degrees of freedom, and for creating nanoelectromechanical systems (NEMS). For example, Refs. [5,6] show that the electron transport through a quantum point contact placed on a micromechanical resonator is sensitive to mechanical vibrations. References [2,7,8] demonstrate that diffusive conductive channels in a 2DEG can also be used as nanoelectromechanical transducers.

The two fundamental key points arising in the context of NEMS are the physical mechanisms underlying actuation and transduction of the nanomechanical motion. The actuation in NEMS with a 2DEG is addressed elsewhere [7], while the present Letter is focused on the transduction mechanism. Most papers considering GaAs/AlGaAs-based suspended systems contain a proposal that a 2DEG embedded in a resonator is sensitive to its vibrations due to the change in the density of a 2DEG that screens the piezoelectrically induced bound charge [2,5,6,9]. However, there is a lack of experimental evidence for this hypothesis and there is seemingly no common physical model describing this electromechanical coupling.

In the present Letter, we experimentally demonstrate that the dominant physical mechanism making a 2DEG sensitive to NEMS mechanical vibrations is associated with the piezoelectric effect and show the sensitivity magnitude. We also propose a physical model giving an independent estimate for the sensitivity magnitude consistent with the experiment. According to the model, the local change in the 2DEG conductivity is determined mainly by spatial deviations of the mechanical stress tensor, rather than by the stress itself, as could be intuitively expected.

The piezoelectric effect is essentially anisotropic [10,11] and, in a GaAs crystal, identical mechanical stresses in the perpendicular directions [110] and [$\bar{1}$10] induce opposite electrical polarizations. The central idea of the experiment is to check whether the change in the conductivity of a 2DEG, contained in two identically vibrating cantilevers oriented in the considered directions, reflects such anisotropy and, thus, to test the hypothesis about the piezoelectric nature of electromechanical coupling.

The experimental samples are fabricated from the GaAs/AlGaAs heterostructure described in detail in Ref. [7]. The heterostructure contains a 166 nm-thick stack of layers grown by means of molecular-beam epitaxy above a 400 nm-thick $Al_{0.8}Ga_{0.2}As$ sacrificial layer, which, in turn, resides on the [001]-oriented GaAs substrate. The stack contains two $Al_{0.33}Ga_{0.67}As$ layers surrounding the 13 nm-thick GaAs layer with a 2DEG. Also, the stack contains a 10 nm-thick GaAs top cap layer. The 2DEG has an electron density of $n = 6.7 \times 10^{11}$ cm^{-2} and the mobility of $\mu = 1.2 \times 10^6$ cm^2 V^{-1} s^{-1}. The samples' lateral geometry is defined using electron-beam lithography followed by anisotropic plasmachemical etching in BCl_3. The samples are suspended using selective wet etching in a 1:100 hydrofluoric acid water solution. The electron

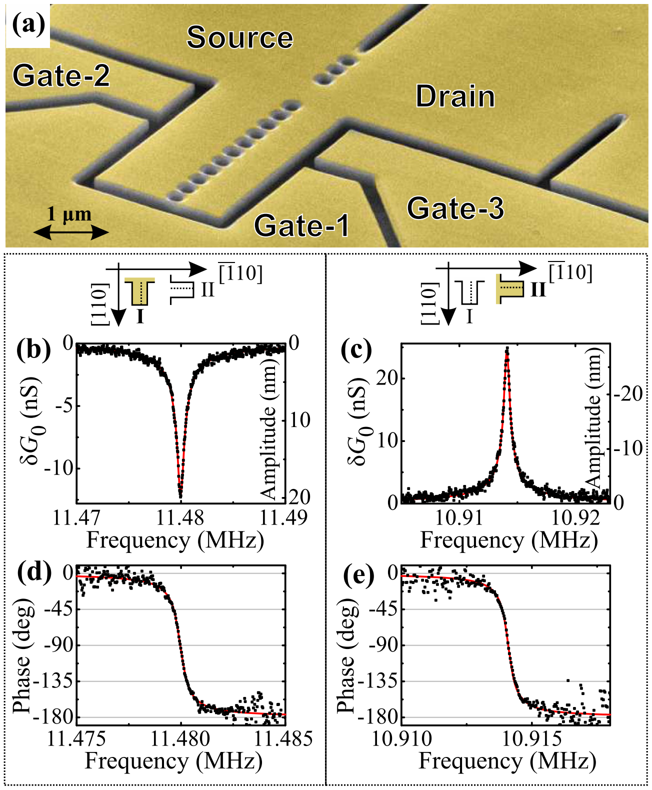

FIG. 1. (a) False-color scanning-electron-microscope image of a cantilever containing a two-dimensional electron gas. The areas between the holes in the cantilever are nonconductive due to edge depletion, except for the one constriction where the interhole distance is enlarged. (b)–(e) Signed amplitudes (b),(c) and phases (d),(e) of the change in the conductance of the cantilevers oriented along [110] (b),(d) and [$\bar{1}$10] (c),(e) crystallographic directions measured at the temperature of 4.2 K.

density was shown [12] earlier to remain almost unchanged after the suspension of a similar heterostructure.

Each experimental chip contains two identical cantilevers oriented in perpendicular directions ([110] and [$\bar{1}$10]). Hereinafter, we will refer to them as Cantilever-I and Cantilever-II, respectively. The cantilevers are $L = 3\ \mu$m long, $W = 2\ \mu$m wide, and $t = 166$ nm thick [see Fig. 1(a)]. There is a series of holes placed on a longitudinal line on each of the cantilevers. The distance between the holes is small enough for the regions between them be nonconductive due to edge depletion, except for one spacing near the cantilever base, where the distance is enlarged up to 600 nm. Thus, the line of holes electrically separates the 2DEG into two areas—the source and the drain (individual for each cantilever)—connected via a single constriction. Each cantilever is equipped with three side gates with one of them (Gate-1) surrounding the free end [see Fig. 1(a)].

The conductance G response to the cantilevers' vibrations is measured using the heterodyne downmixing technique [13] applied in the following way. Consider a cantilever performing small flexural vibrations at the fundamental mode as a driven linear oscillator, the motion of which is described by the following equation:

$$\ddot{\xi} + \frac{\Omega_0}{Q}\dot{\xi} + \Omega_0^2\xi = \frac{F_0 \cos \Omega t}{m}, \quad (1)$$

where ξ is displacement of the cantilever free end, Ω_0 is resonant frequency, Q is the quality factor, F_0 and Ω are the amplitude and the frequency of the effective driving force, and m is the cantilever effective mass. Write the solution of Eq. (1) as

$$\xi = \xi_0(\Omega) \cos [\Omega t + \varphi(\Omega)]. \quad (2)$$

Since the vibrations are small, consider only the linear conductance response to the vibrations:

$$G = G_0 + \frac{dG}{d\xi}\xi = G_0 + \delta G_0 \cos [\Omega t + \varphi(\Omega)]. \quad (3)$$

To transform this high-frequency response into a low-frequency electrical signal, we apply a voltage

$$V_{\mathrm{SD}} = V_0 \cos [(\Omega - \omega)t] \quad (4)$$

between the source and the drain. Here $\omega = 2\pi \times 25$ kHz $\ll \Omega$, Ω_0. Source-drain current $I = GV_{\mathrm{SD}}$ has two components at the high $2\Omega - \omega$ and the low ω heterodyne frequencies. The low-frequency component which we measure in the experiment is

$$I_\omega = I_0(\Omega) \cos [\omega t + \varphi(\Omega)], \quad (5)$$

where $I_0(\Omega) = V_0 \delta G_0(\Omega)/2$. Thus, measuring amplitude $I_0(\Omega)$ and the phase of this low-frequency current, we obtain the amplitude $\delta G_0(\Omega) = 2I_0(\Omega)/V_0$ and the phase $\varphi(\Omega)$ of the high-frequency conductance response to vibrations. At the same time, the heterodyne downmixing eliminates the known difficulties inherent to the measurements at the high driving frequency [13].

The cantilevers' vibrations are driven at the fundamental flexural mode perpendicularly to the surface using the electrostatic (capacitive) actuation scheme. For this purpose, we apply a voltage V_G to Gate-1 [see Fig. 1(a)], satisfying condition $|V_G| \gg |V_{\mathrm{SD}}|$. Then the effective driving force is

$$F = C' V_G^2/2, \quad (6)$$

where factor C' is proportional to the derivative of the gate-cantilever capacitance on the free end displacement ξ (we assume $\xi > 0$ if the cantilever is bent up in the direction from the substrate). As shown in Ref. [7], C' can be estimated as

$$C' \approx -0.39\varepsilon_0 WL/d_0^2, \quad (7)$$

where ε_0 is the vacuum dielectric constant and $d_0 = 400$ nm is the distance between the cantilever and the underlying substrate.

The applied voltage V_G is a sum of dc and ac components:

$$V_G = V_{\rm dc} + V_{\rm ac} \cos[(\Omega - \omega)t] \times [1 + \cos \omega t]. \quad (8)$$

The ac component is a high-frequency signal (proportional to $V_{\rm SD}$) amplitude-modulated by low frequency ω. The modulated signal has three components: one at carrier frequency $\Omega - \omega$ and two at sidebands $\Omega - 2\omega$ and $\Omega \approx \Omega_0$. The effective force acting at the frequency Ω obtained from Eqs. (6) and (8) has the amplitude

$$F_0 = C' V_{\rm dc} V_{\rm ac}/2. \quad (9)$$

Since, as we show later, $\omega \gg \Omega_0/Q$, the other frequency components of the effective force are far from the resonance and can be neglected.

We use a Tektronix AFG3252C two-channel generator and appropriate attenuators to apply the gate and source-drain voltages. The modulating signal is applied to the generator input from an SR5210 lock-in amplifier. The lock-in amplifier is also used to measure the amplitude $I_0(\Omega)$ and the phase $\varphi(\Omega)$ of the current I_ω. The phase is measured with respect to the modulating signal. During the experiment, the samples are placed in a vacuum tube and cooled down to liquid helium temperature 4.2 K.

Figures 1(b) and 1(c) show the signed amplitude $\delta G_0(\Omega)$ of the conductance response measured as a function of driving frequency $\Omega/2\pi$ for the Cantilever-I and Cantilever-II, respectively. Phase $\varphi(\Omega)$ is shown in Figs. 1(d) and 1(e). The curves are obtained at $V_{\rm dc} = 2$ V, $V_{\rm ac} = 50$ mV and $V_0 = 6.25$ mV.

The main difference between the data obtained for the perpendicularly oriented cantilevers is the sign of their electrical response to vibrations. This difference could equivalently be shown by a 180° phase shift, but we use the signed amplitude for clarity. The amplitude-frequency dependence has a Lorentzian form and agrees with Eqs. (1) and (3), as well as the measured phase-frequency dependence. The solid red lines in Figs. 1(b)–(e) show the corresponding fits to the experimental data. The resonant frequencies $\Omega_0/2\pi$ extracted from the fits are 11.455 MHz and 10.889 MHz for the Cantilever-I and Cantilever-II, respectively. Quality factors Q are 18 000 and 23 400. The measured resonant frequencies agree with the rough estimate [14] $\Omega_0/2\pi = 0.16t\sqrt{E/\rho}/L^2 \approx 14.8$ MHz, which can be obtained for the first flexural mode of thin cantilever vibrations. Here $E = 121$ GPa is the [110] Young modulus of $Al_{0.33}Ga_{0.67}As$ [15] and $\rho = 4800$ kg/m^3 is the mass density. Some discrepancy can be explained by the fact that the cantilevers' width is not small in comparison with their length, as well as by their nonuniformity and by the etching undercut.

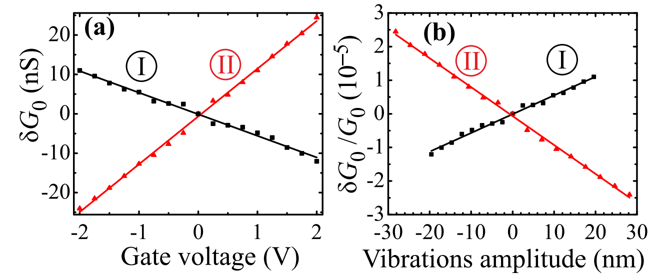

FIG. 2. (a) The signed amplitudes of the conductance change induced by vibrations have the opposite signs for the Cantilever-I and the Cantilever-II in all of the gate voltage range. (b) Relative amplitude of the conductance change as a function of the estimated vibrations' amplitude.

Consider the factors influencing the sign of $\delta G_0(\Omega_0)$. This resonant amplitude of the conductance change is proportional to the vibrations amplitude which, in turn, can be expressed from Eqs. (1) and (9) as

$$\xi_0(\Omega_0) = \frac{F_0 Q}{m\Omega_0^2} = \frac{C' V_{\rm dc} V_{\rm ac} Q}{2m\Omega_0^2}. \quad (10)$$

Thus, $\delta G_0(\Omega_0)$ should be proportional to $V_{\rm dc}$ and should change the sign with its negation, if the vibrations are electrostatically driven. Figure 2(a) shows the experimentally measured $\delta G_0(\Omega_0)$ dependence on $V_{\rm dc}$. The shown data confirm the predicted behavior, with $\delta G_0(\Omega_0)$ having opposite signs for the two cantilevers in all the range of $V_{\rm dc}$. Since the sign of $\xi_0(\Omega_0)$ does not depend on crystallographic orientation, the observed negation of $\delta G_0(\Omega_0)$, according to Eq. (3), shows that $dG/d\xi$ has the opposite signs for the cantilevers oriented in [110] and $[\bar{1}10]$ directions. This anisotropy can be considered as indicative of the piezoelectric nature of the mechanical vibrations' influence on the conductance. To obtain an additional quantitative confirmation of this hypothesis and to reveal the details of piezoelectric response, we have compared independent experimental and numerical estimates of the relative sensitivity to the vibrations $(1/G_0)(dG/d\xi)$. This value is the proportionality factor between the relative conductance change and the vibrations' amplitude:

$$\frac{\delta G_0(\Omega_0)}{G_0} = \frac{1}{G_0}\frac{dG}{d\xi}\xi_0(\Omega_0). \quad (11)$$

The $\delta G_0(\Omega_0)/G_0$ dependence on $\xi_0(\Omega_0)$ estimated using Eq. (10) is shown in Fig. 2(b). The cantilevers' resistance $1/G_0$ calculated as a difference between measured two-terminal resistance and estimated lead resistance (300 Ω) equals 1 kΩ. A cantilever effective mass appearing in Eq. (10) is estimated as $m = 0.24\rho tWL$ [7]. The data shown in Fig. 2(b) give the desired values of $(1/G_0)(dG/d\xi)$ equal to 5.6×10^{-4} μm^{-1} and -8.6×10^{-4} μm^{-1} for the Cantilever-I and the Cantilever-II, respectively. The observed behavior is reproduced on another sample giving

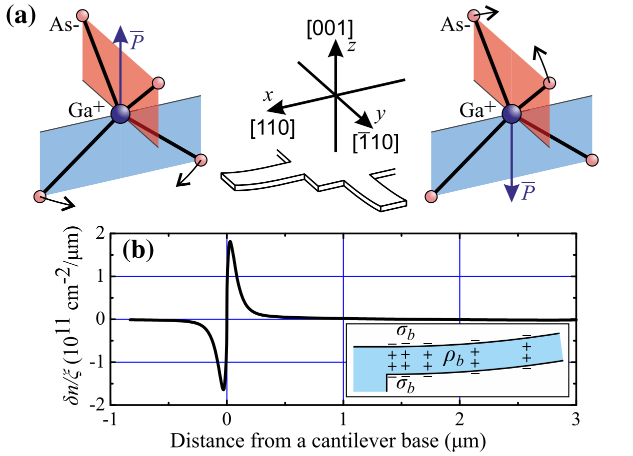

FIG. 3. (a) Simplified picture showing the origin of the piezoelectric response anisotropy. (b) Spatial dependence of the estimated change in electron density δn per unit displacement ξ of the cantilever free end. The shown dependence corresponds to the [110]-oriented cantilever and should be negated for the $[\bar{1}10]$-oriented cantilever.

the sensitivity values $7\times10^{-4}\ \mu\mathrm{m}^{-1}$ and $-11\times10^{-4}\ \mu\mathrm{m}^{-1}$. The rest of the Letter is devoted to a physical model giving an independent estimate for this value.

To roughly estimate the mechanical stress, we use the Euler-Bernoulli beam theory and neglect the fact that the cantilevers' width $W = 2\ \mu$m is not much less than their length $L = 3\ \mu$m. The shape of the first flexural mode is [7,14]

$$U = \xi\times[A(\cos kl - \cosh kl) + B(\sin kl - \sinh kl)] \tag{12}$$

where l is the distance from a cantilever base, $k \approx 1.875/L$, $A \approx -0.5$ and $B \approx 0.367$. We introduce x, y, and z axes coinciding with [110], $[\bar{1}10]$, and [001] crystallographic directions, respectively [see Fig. 3(a)]. Then the six-dimensional vectors [16] describing the mechanical stress (in Voigt notation) are

$$\sigma_i^I = (\sigma\quad 0\quad 0\quad 0\quad 0\quad 0)^T,$$
$$\sigma_i^{II} = (0\quad \sigma\quad 0\quad 0\quad 0\quad 0)^T \tag{13}$$

for the Cantilever-I and the Cantilever-II. Here

$$\sigma = -Ezd^2U/dl^2, \tag{14}$$

where $z = 0$ corresponds to the cantilever neutral plane. The piezoelectric effect leads to electrical polarization $P_i = d_{ij}\sigma_j$, where d_{ij} is the piezoelectric matrix [16]:

$$d_{ij} = d_{14}\begin{pmatrix} 0 & 0 & 0 & 0 & 1 & 0\\ 0 & 0 & 0 & -1 & 0 & 0\\ 1 & -1 & 0 & 0 & 0 & 0\end{pmatrix}. \tag{15}$$

Here $d_{14} = -3.04$ pm/V for $Al_{0.33}Ga_{0.67}As$ [15]. This nonuniform polarization induces the volume bound charge with the density

$$\rho_b = -\mathrm{div}\boldsymbol{P} = \mp d_{14}\frac{d\sigma}{dz} = \mp d_{14}E\frac{d^2U}{dl^2}, \tag{16}$$

where signs "−" and "+" correspond to the Cantilever-I and the Cantilever-II, respectively [see Fig. 3(a)]. The volume charge is compensated by the bound charge

$$\sigma_b = -\rho_b t/2 \tag{17}$$

on the upper and lower surfaces of the cantilever.

Let the electrical potential created by the bound charge be $\delta\phi_{\mathrm{ext}}$. The 2DEG responds to this external influence with a change in electron density δn, which, in turn, leads to the change in chemical potential $\delta n\pi\hbar^2/m^*$ and to the change in electrical potential $\delta\phi_{\mathrm{resp}}$, such that the electrochemical potential remains zero:

$$-e(\delta\phi_{\mathrm{ext}} + \delta\phi_{\mathrm{resp}}) + \delta n\frac{\pi\hbar^2}{m^*} = 0. \tag{18}$$

Here e and m^* are negated electron charge and effective mass in GaAs. To estimate δn, we neglect the last term in Eq. (18), assume pure electrostatic screening [17] and the 2DEG having constant electrical potential $\delta\phi_{\mathrm{ext}} + \delta\phi_{\mathrm{resp}} = 0$. This assumption is reasonable if

$$|\delta n\pi\hbar^2/m^*| \ll |e\delta\phi_{\mathrm{ext}}|. \tag{19}$$

To understand this, consider the influence of a point charge q at the distance r from the 2DEG. The induced δn is of order of $q/(er^2)$, and $\delta\phi_{\mathrm{ext}} \approx q/(4\pi\varepsilon\varepsilon_0 r)$. The substitution of these expressions into Eq. (19) shows its equivalence to condition $r \gg a_B$, where $a_B \approx 13$ nm is the effective Bohr radius in GaAs, much less than membrane thickness $t = 166$ nm. Thus, we believe that the model of pure electrostatic screening allows us to estimate the influence of most of the bound charge induced by a cantilever bending.

For simplicity, we consider the system as an infinite nonbent equipotential plane (2DEG) sandwiched between two $t/2$-thick layers of a material with dielectric constant $\varepsilon \approx 13$ equal to that of $Al_{0.33}Ga_{0.67}As$. We neglect the small bending in electrostatic calculations, but save the bound charge determined by Eqs. (16) and (17) at $0 \le l \le L$. Using these simplifications, we estimate the screening charge density using the method of images:

$$\delta n = -\frac{1}{2\pi e}\int_0^L \rho_B\left[f_{\mathrm{surf}}\left(\frac{l-l'}{t}\right) + f_{\mathrm{vol}}\left(\frac{l-l'}{t}\right)\right]dl', \tag{20}$$

where

$$f_{\mathrm{surf}}(r) = \frac{2\varepsilon}{\varepsilon+1}\sum_{n=0}^{\infty}\left(-\frac{\varepsilon-1}{\varepsilon+1}\right)^n\frac{n+1/2}{r^2+(n+1/2)^2}, \tag{21}$$

$$f_{\mathrm{vol}}(r) = -\ln\left(1+\frac{1}{4r^2}\right) - \sum_{n=1}^{\infty}\left(-\frac{\varepsilon-1}{\varepsilon+1}\right)^n \ln\frac{[r^2+(n+1/2)^2][r^2+(n-1/2)^2]}{[r^2+n^2]^2} \tag{22}$$

The calculated δn per unit displacement of the cantilever free end ξ is shown in Fig. 3(b) as a function of distance l from the cantilever base. The obtained dependence shows that the considered effect is expected to be most prominent at distances $|l|$ of the order of the cantilever thickness t from its base, with δn changing the sign when l is negated. Almost the same dependence can be obtained for the mechanical stress in the form of $\sigma(l=0)\Theta(l)$, where σ is determined by Eq. (14) and $\Theta(l)$ is the Heaviside step function. This shows that, the change in electron density $\delta n(l)$ is primarily an edge effect arising near the point $l=0$, where the stress suffers a jump. This point corresponds to the lateral boundary between suspended and nonsuspended areas. Actually $\sigma(l)$ decreases rapidly in the nonsuspended bulk at the characteristic distance of order t from the boundary. Thus, the stepwise jump of the mechanical stress implied by our model can be used as a reasonable simplification.

The cantilever is thin enough (166 nm) for the considered boundary to be clearly seen with a scanning electron microscope. The measured distance between the boundary and the constriction center equals $l = 1.3$ μm. The electron density change corresponding to this distance can be obtained from Eq. (20) and equals $d(\delta n)/d\xi = 7.4\times 10^8$ cm^{-2} μm^{-1}. We neglect the periodic influence of the vibration-induced stress on the electron mobility [18], because the 2DEG placed closely to the cantilever neutral plane is almost not subject to the stress. Moreover, the characteristic time of impurity recharging far exceeds the vibration period. Then the expected relative conductance sensitivity to the vibrations is equal to the expected relative change in the electron density: $(1/G_0)(dG/d\xi) = (1/n)\big(d(\delta n)/d\xi\big) \approx 1.1\times 10^{-3}$ μm^{-1}. This value agrees with the values 0.56×10^{-3} μm^{-1} and -0.86×10^{-3} μm^{-1} experimentally obtained above for the Cantilever-I and Cantilever-II. Thus, the proposed model agrees with the experiment and describes it adequately, though a detailed experimental study of the spatial change in the electron density near the boundary between suspended and nonsuspended areas is desirable.

To conclude, it is experimentally shown that the conductance change resulting from mechanical vibrations of NEMS with a 2DEG demonstrates the anisotropy inherent to a piezoelectric effect. A model describing this change and predicting its value is proposed. The model implies that the mechanical stress induces the bound charge which is screened by the change in the 2DEG density. According to the model, the change in 2DEG conductivity is related primarily to the rapid change in the mechanical stress near the boundary between suspended and nonsuspended areas, rather than to the stress itself.

We thank Tektronix corporation, Alpha-instruments company, and Ilya Dianov for providing an AFG3252C arbitrary form generator. The work is supported by RFBR Grants No. 16-32-60130, No. 15-02-05774, and No. 16-02-00579.

*shevandrey@isp.nsc.ru

[1] R. Blick, M. Roukes, W. Wegscheider, and M. Bichler, Physica (Amsterdam) **249B–251B**, 784 (1998).

[2] H. X. Tang, X. M. H. Huang, M. L. Roukes, M. Bichler, and W. Wegscheider, Appl. Phys. Lett. **81**, 3879 (2002).

[3] I. Mahboob, K. Nishiguchi, A. Fujiwara, and H. Yamaguchi, Phys. Rev. Lett. **110**, 127202 (2013).

[4] A. D. O'Connell, M. Hofheinz, M. Ansmann, R. C. Bialczak, M. Lenander, E. Lucero, M. Neeley, D. Sank, H. Wang, M. Weides, J. Wenner, J. M. Martinis, and A. N. Cleland, Nature (London) **464**, 697 (2010).

[5] A. N. Cleland, J. S. Aldridge, D. C. Driscoll, and A. C. Gossard, Appl. Phys. Lett. **81**, 1699 (2002).

[6] Y. Okazaki, I. Mahboob, K. Onomitsu, S. Sasaki, and H. Yamaguchi, Appl. Phys. Lett. **103**, 192105 (2013).

[7] A. A. Shevyrin, A. G. Pogosov, M. V. Budantsev, A. K. Bakarov, A. I. Toropov, E. E. Rodyakina, and A. A. Shklyaev, Appl. Phys. Lett. **106**, 183110 (2015).

[8] A. A. Shevyrin, A. G. Pogosov, M. V. Budantsev, A. K. Bakarov, A. I. Toropov, S. V. Ishutkin, E. V. Shesterikov, and A. S. Arakcheev, Appl. Phys. Lett. **103**, 131905 (2013).

[9] R. G. Beck, M. A. Eriksson, M. A. Topinka, R. M. Westervelt, K. D. Maranowski, and A. C. Gossard, Appl. Phys. Lett. **73**, 1149 (1998).

[10] S. C. Masmanidis, R. B. Karabalin, I. D. Vlaminck, G. Borghs, M. R. Freeman, and M. L. Roukes, Science **317**, 780 (2007).

[11] E. A. Vopilkin, V. I. Shashkin, Y. N. Drozdov, V. M. Daniltsev, S. A. Gusev, and I. Y. Shuleshova, J. Micromech. Microeng. **18**, 095006 (2008).

[12] A. G. Pogosov, M. V. Budantsev, E. Y. Zhdanov, D. A. Pokhabov, A. K. Bakarov, and A. I. Toropov, Appl. Phys. Lett. **100**, 181902 (2012).

[13] I. Bargatin, E. B. Myers, J. Arlett, B. Gudlewski, and M. L. Roukes, Appl. Phys. Lett. **86**, 133109 (2005).

[14] L. D. Landau and E. M. Lifshitz, *Theory of Elasticity,* A Course of Theoretical Physics Vol 7 (Pergamon Press, New York, 1970).

[15] S. Adachi, J. Appl. Phys. **58**, R1 (1985).

[16] J. F. Nye, *Physical Properties of Crystalls* (Oxford University Press, London, 1985).

[17] J. H. Davies and I. A. Larkin, Phys. Rev. B **49**, 4800 (1994).

[18] C. T. Leondes, *MEMS/NEMS Handbook. Techniques and Applications* (New York, Springer, 2006), Vol. 1.